New 7-azaindole palladium and platinum complexes: crystal structures and theoretical calculations. *In vitro* anticancer activity of the platinum compounds†

José Ruiz,*[a] Venancio Rodríguez,[a] Concepción de Haro,[a] Arturo Espinosa,*[b] José Pérez[c] and Christoph Janiak[d]

Received 7th October 2009, Accepted 15th January 2010
First published as an Advance Article on the web 13th February 2010
DOI: 10.1039/b920854b

A series of new 7-azaindolyl palladium and platinum complexes have been prepared. The X-ray structure determinations of $[NBu_4][M(C_6F_5)_2(Haza\text{-}N7)(aza\text{-}N1)]\cdot Haza$ [M = Pd, Pt; aza = 7-azaindolate (1*H*-pyrrolo[2,3-*b*]pyridinate)] have established for the first time the coordination to the same metal centre of both neutral and anionic forms of the ligand. Theoretical calculations at the mPW1B95/aug6-31G**/StRSCecp level show that both kinetic and thermodynamic arguments support the observed coordination and H-bonding interaction of the pyrrolo and pyridine moieties of the neutral and deprotonated heterocyclic ligands. At 48 h incubation time the new platinum complex [Pt(dmba)(aza-N1)(DMSO)] (dmba = *N*,*N*-dimethylbenzylamine-κN,κC) shows sub-micromolar activity both in A2780 and T47D [IC_{50} (μM) = 0.34 and 0.53, respectively]. The DNA adduct formation of the new platinum complexes was followed by circular dichroism and electrophoretic mobility.

Introduction

Multidentate nitrogen-donor ligands are designed with the aim of preparing polynuclear compounds with an appropriate metal–metal separation, which is very important in studies of functional models for bimetallic biosites.[1] Such ligands are also extensively used for the assembly of cyclic supermolecules,[2–7] the preparation and characterization of polynuclear metal complexes and their potential use for the study of multi-centered catalysis.[8] Recent reports by Reedijk *et al.* have shown that the azolate-bridged dinuclear platinum(II) complexes, $[\{cis\text{-}Pt(NH_3)_2\}_2(\mu\text{-}OH)(\mu\text{-}pz)](NO_3)_2$ (pz = pyrazolate) and $[\{cis\text{-}Pt(NH_3)_2\}_2(\mu\text{-}OH)(\mu\text{-}1,2,3\text{-}tz\text{-}N1,N2)](NO_3)_2$ (1,2,3-tz = 1,2,3-triazolate), exhibit remarkably high *in vitro* cytotoxicity on several human tumour cell lines and largely circumvent the cross-resistance to cisplatin.[9–11] Metal 7-azaindolate (aza) complexes have also attracted considerable interest in recent years due to their versatile coordination chemistry.[12–15] In the 7-aza ligand the donor atoms are in rigid positions, although they have a large bite angle (Chart 1).

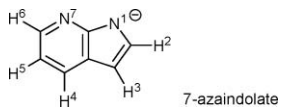

Chart 1

In this article we describe the synthesis of 7-azaindolyl metal complexes of the types [M(dmba)(aza-N1)(L)], $[M(C_6F_5)_2(Haza\text{-}N7)_2]$ and $[NBu_4][M(C_6F_5)_2(Haza\text{-}N7)(aza\text{-}N1)]\cdot Haza$ [M = Pd, Pt; aza = 7-azaindolate (1*H*-pyrrolo[2,3-*b*]pyridinate); dmba = *N*,*N*-dimethylbenzylamine-κN,κC], the latter exhibiting for the first time the coordination to the same metal centre of both neutral and anionic forms of the ligand according to a search of the Cambridge Structure Database (CSD)[16] and a survey of recent literature in SciFinder® Scholar. The azaindolate-bridged dinuclear complexes $[NBu_4]_2[\{cis\text{-}M(C_6F_5)_2\}_2(\mu\text{-}OH)(\mu\text{-}aza\text{-}N1,N7)]$ (M = Pd, Pt) have also been prepared. Calculations by means of DFT-based calculations at the BP86/def2TZVP level have been undertaken. Values of IC_{50} were studied for the new platinum complexes against a panel of human tumor cell lines representative of ovarian (A2780 and A2780*cis*R), and breast cancers (T47D, cisplatin resistant). The DNA adduct formation of the new platinum complexes is also reported.

Results and discussion

Neutral bis(7-azaindolyl) complexes *cis*-$[M(C_6F_5)_2(Haza\text{-}N7)_2]$

The reaction of $[M(C_6F_5)_2(PhCN)_2]$[17,18] (M = Pd, Pt) with Haza in the molar ratio 1 : 2 gives the corresponding bis(7-azaindolyl) complex of $[M(C_6F_5)_2(Haza\text{-}N7)_2]$ **1–2** (Scheme 1). The reactions

[a]*Departamento de Química Inorgánica, Facultad de Química, Universidad de Murcia, 30071, Murcia, Spain. E-mail: jruiz@um.es; Fax: +34 868 384148; Tel: +34 868 887455*
[b]*Departamento de Química Orgánica, Facultad de Química, Universidad de Murcia, 30071, Murcia, Spain. E-mail: artuesp@um.es; Fax: +34 868884149; Tel: +34 868 887489*
[c]*Departamento de Ingeniería Minera, Geológica y Cartográfica (Área de Química Inorgánica), Universidad Politécnica de Cartagena, 30203-, Cartagena, Spain. E-mail: Jose.Pperez@upct.es; Fax: +34 968 325420; Tel: +34 968 326420*
[d]*Institut für Anorganische und Analytische Chemie, Universität Freiburg, Albertstr., 21, 79104, Freiburg, Germany. E-mail: janiak@uni-freiburg.de; Fax: +49 761 2036147; Tel: +49 761 2036127*

† Electronic supplementary information (ESI) available: Figures illustrating the molecular structure of 1, the toluene disorder in **9**, the TGA-DTA of complexes **3** and **4** and other significant MO in $\mathbf{6}^{calc}$. Cartesian coordinates and energies for all calculated species and HSAB-derived parameters for the reaction of **7** with aza. CCDC reference numbers 717464–717466 and 750363. For ESI and crystallographic data in CIF format see DOI: 10.1039/b920854b

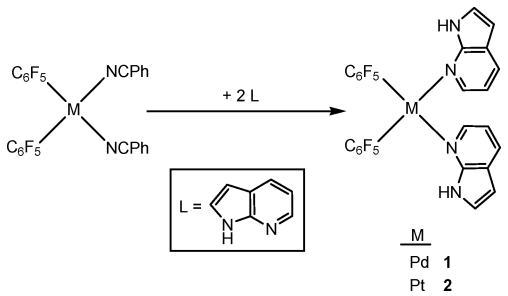

Scheme 1

take place without isomerization, and the reaction products are the *cis* isomers. Their IR spectra show the characteristic absorptions of the C_6F_5 group (1630 m, 1490 vs, 1050 s, and 950 vs cm^{-1})[19] and a split band at *ca.* 800 cm^{-1} assigned to the *cis*-$M(C_6F_5)_2$ moiety.[20–24] The ^{19}F NMR spectra of **1** and **2** show the expected three signals for two equivalent C_6F_5 rings with relative intensities of $2F_o$:$1F_p$:$2F_m$. As expected, the *ortho*-F signals of complex **2** are flanked by satellites due to coupling to ^{195}Pt. The ^1H spectrum of complex **2** in $CDCl_3$ at room temperature exhibits an unique set of resonances for both heterocyclic ligands, no changes being observable over the −50 to +50 °C range. The resonance at δ 8.30 ppm for complex **2** should be assigned to 6-H because this signal is flanked by ^{195}Pt satellites in the spectrum. Furthermore, the rest of assignments given in the Experimental for complexes **1** and **2** were also supported by the pertinent homonuclear (^1H–^1H) COSY spectra.

The final confirmation of the nature of **1** was obtained by an X-ray diffraction study. From the data available, the molecular skeleton can be established (ESI, Fig. S1).†[25] The two possible dispositions H–H and H–T (Fig. 1) of the azaindole ligands create, however, an inherent disorder problem.

Compounds $[NBu_4][M(C_6F_5)_2(Haza\text{-}N7)(aza\text{-}N1)]\cdot Haza$ and $[NBu_4]_2[\{M(C_6F_5)_2\}_2(\mu\text{-}OH)(\mu\text{-}aza\text{-}N7,N1)]$ (M = Pd, Pt)

Compounds $[NBu_4][M(C_6F_5)_2(Haza\text{-}N7)(aza\text{-}N1)]\cdot Haza$ [M = Pd (**3**), Pt (**4**)] can be prepared from **1** or **2** and NBu_4OH in the presence of excess Haza (Scheme 2). They contain simultaneously both the neutral Haza and the anionic aza ligands, and a Haza molecule of crystallization. Compounds **3** and **4** are stable up to

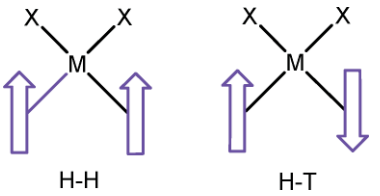

Fig. 1 The two possible atropisomers in square-planar metal complexes containing two equal planar ligands occupying *cis* coordination positions.

about 100 °C where decomposition with loss of all the (H)aza groups starts (ESI, Fig. S3 and S4).† The reaction of **1** or **2** with NBu_4OH in the absence of additional Haza yielded only a mixture of the starting material with **3** or **4**, respectively. The palladium compound **3**, alternatively, can also be prepared from the hydroxo palladium complex $[NBu_4]_2[Pd(C_6F_5)_2(\mu\text{-}OH)]_2$[18] and Haza in a 1 : 8 molar ratio. The reaction of $[NBu_4]_2[M(C_6F_5)_2(\mu\text{-}OH)]_2$[18,26] with Haza (in a 1 : 1 molar ratio for Pd, 1 : 2 molar ratio for Pt) yields the corresponding azaindolate dinuclear complex $[NBu_4]_2[\{M(C_6F_5)_2\}_2(\mu\text{-}OH)(\mu\text{-}aza\text{-}N7,N1)]$ [M = Pd (**5**), Pt (**6**)].

The ^1H NMR spectra of **3** and **4** in CD_2Cl_2 at room temperature exhibit three different sets of resonances with relative intensities 1 : 1 : 1 for the three different 7-azaindolyl groups. The assignments given in the Experimental for complexes **3** and **4** were supported by the homonuclear (^1H–^1H) COSY spectra and, in the case of complex **4**, take into account that some resonances (H2 or H6 of the coordinated azaindolyl ligands) are flanked by ^{195}Pt satellites. The ^{19}F NMR patterns of **3** and **4** are consistent with the presence of two non-equivalent C_6F_5 groups, one C_6F_5 *trans* to aza and one C_6F_5 *trans* to Haza.

The ^1H NMR spectra in $CDCl_3$ of **5** and **6** are consistent with the bridging azaindolate ligand and only one set of signals is observed for the protons of the heterocyclic moiety. The presence of the OH group in complexes **5** and **6** is demonstrated by the high-field ^1H resonance observed at δ −1.34 and −0.12 ppm for **5** and **6**, respectively, as well as the ν(OH) band observed at *ca.* 3600 cm^{-1}.

Crystal structures of azaindole-azaindolate compounds 3 and 4

The structures of $[NBu_4][M(C_6F_5)_2(Haza\text{-}N7)(aza\text{-}N1)]\cdot Haza$ (**3**, **4**) were isomorphous, and both compounds crystallized in a monoclinic unit cell, space group $P2_1/c$. The structure of the

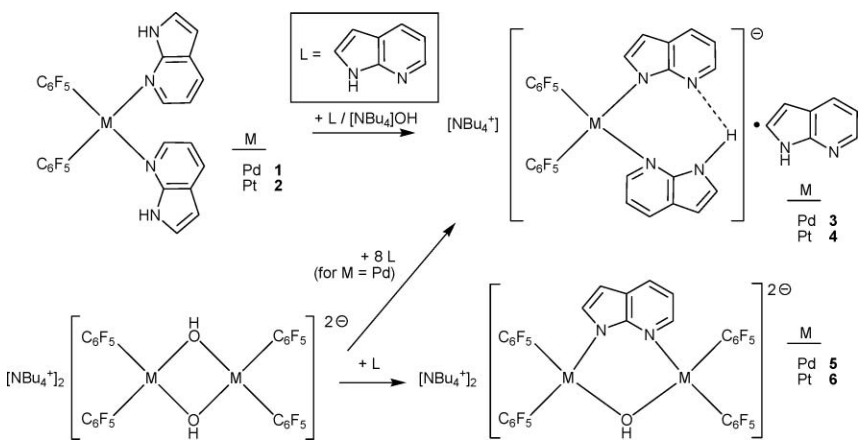

Scheme 2

anion of **3** is shown in Fig. 2. The coordination at palladium and platinum is square-planar with interbond angles which deviate little from 90° (Table 1). The neutral azaindole ligand (Haza) binds through its pyridine nitrogen atom, the anionic azaindolate ligand (aza) through its pyrrole nitrogen atom to the metal atom. In the crystal, there is an intramolecular N–H···N contact between the two coordinated azaindolyl groups (Fig. 2), which is certainly responsible for the orientation of the pyrrolo and the pyridine moieties of the two ligands. The asymmetric intramolecular N–H···N contact observed in **3** and **4** contrasts with the symmetric intramolecular interactions previously found in the related complexes $[NBu_4][M(C_6F_5)_2$-(pyrazole)(pyrazolate)] (M = Pd, Pt),[24] where the hydrogen atom was located in a symmetric position. Two inversion-related free 7-azaindol molecules of crystallization enter in intermolecular head-to-tail N–H···N contacts with a $R_2^2(8)$ motif, identical to the common complementary carboxylic acid-carboxylic acid graph-set motif (Fig. 3 for **3**).[27–29] A π-stacking interaction between one of the electron-poor C_6F_5 ligands and the azaindole of crystallization is also observed (Fig. 3 for complex **3**), showing a rather short centroid–centroid contact (Ct···Ct < 3.7 Å) between the slightly tilted ring planes (interplanar angle 9.2° and centroid-to-plane separation 3.3 Å for **3**).[30] Other intermolecular interaction contacts observed are of the type C–H···F–C.[31–35] Thus, for example, there are intermolecular C–H···F hydrogen bonding between fluorine atoms of the fluorophenyl groups and hydrogen atoms of NBu_4^+, with the five shortest hydrogen bonds in complex **3** being F7···H41B F5···H33A, F6···H36A, F8···H38C, and F3···H40B (2.45, 2.48, 2.51, 2.54 and 2.54 Å, respectively). Also short C–H···π contacts between NBu_4^+ (H34B in complex **3**) and one of the C_6F_5 rings (C5 in complex **3**) or C–H···π_{aza} contacts have been found.[23,36,37]

The metal–C_6F_5 bond lengths are in the range found in the literature for pentafluorophenyl metal complexes.[15,21,31,37–39]

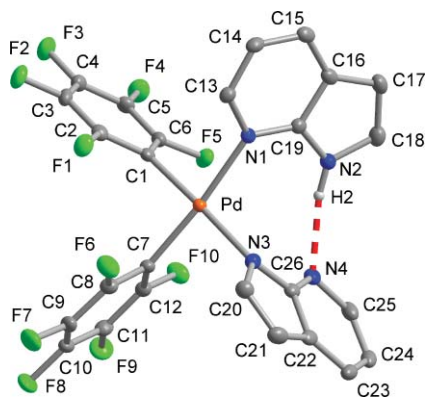

Fig. 2 ORTEP representation (50% probability) of the complex anion of **3** (isostructural to **4**). Hydrogen bonding interaction as dashed line (see Table 1). Hydrogen atoms on carbon have been omitted for clarity.

Theoretical calculations on the platinate anion of 4

The two different binding modes exhibited by ligands Haza and aza in the metallate complexes of **3** and **4** deserve a more detailed analysis with the help of theoretical calculations. We have conducted this study only on the platinum anion (later the π-stacked Haza unit is included), $[Pt(C_6F_5)_2$(Haza-N7)(aza-N1)]$^-$ (**8**)), that

Table 1 Selected bond lengths and angles for **3** and **4**

	3	**4**	**4**$^{calcd\,a}$
M–C1	2.012(2)	2.012(2)	2.022
M–C7	2.005(2)	2.005(2)	2.005
M–N1	2.116(2)	2.099(2)	2.133
M–N3	2.079(2)	2.071(2)	2.119
N2–H2	0.87(3)	0.82(3)	1.053
H2···N4	1.97(3)	2.05(3)	1.846
N2···N4	2.825(3)	2.824(3)	2.838
C7–M–C1	86.28(8)	87.65(9)	90.98
C1–M–N3	175.91(8)	176.63(8)	179.35
C7–M–N3	90.83(7)	90.26(8)	88.84
C1–M–N1	88.65(7)	88.48(8)	87.75
C7–M–N1	174.47(7)	175.76(8)	177.24
N3–M–N1	94.34(7)	93.68(7)	92.41
N2–H2···N4	166(2)	158(3)	155.46

[a] **4**^{calcd} = $[M(C_6F_5)_2$(Haza-N7)(aza-N1)]$^-$·Haza.

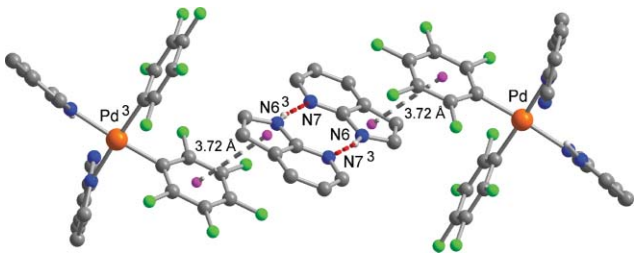

Fig. 3 π-Stacking interaction and intermolecular N–H···N contacts in **3**. Hydrogen bonding interaction (dashed line) [Å, °] in **3**: N6–H 0.91(3), H···N7^3 1.97(3), N6···N7^3 2.863(3), N6–H···N7^3 166(2); corresponding interaction in **4**: 0.99(3), 1.89(3), 2.859(3), 167(2); symmetry relation 3 = 1 − *x*, −*y*, 2 − *z*.

can be considered as formally derived from a neutral unsaturated $[Pt(C_6F_5)_2]$ species through coordination with neutral Haza and anionic aza ligands (Scheme 3). The Haza ligand features only one possible donor atom and therefore is bound to Pt through the pyridine N7 atom, leading to the hypothetical still unsaturated $[Pt(C_6F_5)_2$(Haza-N7)] species **7** (Scheme 3). Finally, binding of the azaindolate anion to the Pt atom in **7** could be achieved through the pyrrole N1 or the pyridine N7 atom, thus leading to **8** or the regioisomeric symmetric complex **8**^{isom}, respectively. A simple analysis regarding the final model compounds points to the expected complex **8** as the thermodynamically controlled product (by only 2.09 kcal mol^{-1}) in the potential energy surface at the working level of theory.

Nevertheless, during the last two decades many important concepts and parameters related to chemical reactivity have been rationalized within the framework of DFT.[40] The DFT formulation[41] of the Pearson's hard–soft acid–base (HSAB) principle[42] states that the most favourable interaction occurs when the reactants have equal softness, provided that the charge reshuffling step can be neglected. The best suited *local* reactivity index for studying regioselectivity[43] is local softness $s(\mathbf{r})$, easily obtained from the Fukui function $f(\mathbf{r})$, defined by Parr and Yang,[44] and the global softness $S = (\partial N/\partial \mu)_{v(\mathbf{r})}$, which describes the ability of the molecule to take or loose electrons in response to a change in the chemical potential, μ. Therefore $s(\mathbf{r})$ describes both the charge transfer between the reactants and how charge is redistributed within the reactants themselves. A local HSAB principle can

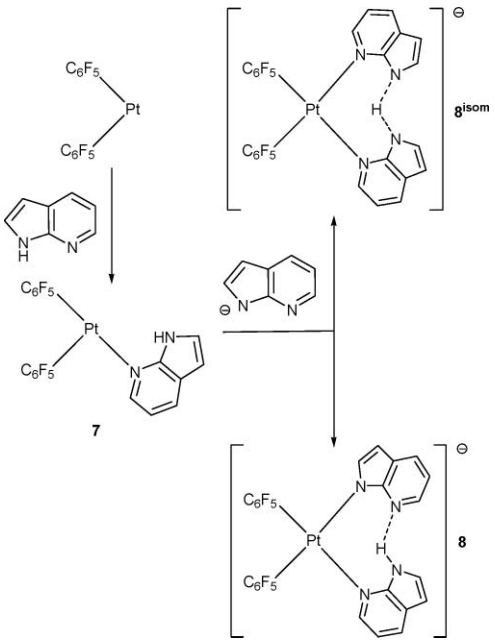

Scheme 3

then be devised as follows: a regioisomer is favoured when the new bond is formed between atoms of equal softness. In other words, the preferred regioisomer in the reaction between atom *k* in molecule A and molecule B will be formed on reaction at atom *l* that minimizes the quadratic difference in local condensed-to-atom softness function[45] $\Delta(s^2)_{kl} = (s_{Ak} - s_{Bl})^2$. An analogous parameter $\Delta(\omega^2)_{kl} = (\omega_{Ak} - \omega_{Bl})^2$ has been proposed,[46] based on local philicities $\omega(\mathbf{r})$ which, in turn, can be easily calculated—*via* Fukui functions $f(\mathbf{r})$—from the global philicity[47] $\omega = \mu^2 S$, measuring the stabilization in energy when the system acquires an additional electronic charge, ΔN, from the environment. For situations in which condensed local softness or philicity were found inadequate to provide the correct intermolecular reactivity trends, the group softness,[48] $s_{(k)g}$, and group philicity,[49] $\omega_{(k)g}$, descriptors have been highlighted, which are obtained after summing the condensed local property—softness or philicity—over all of the *n* neighbouring atoms attached to the reactive site *k*. With this aim we have computed both quadratic-difference parameters for the nucleophilic attack of the two possible donor atoms N1 and N7 in the anionic ligand 7-azaindolate, to the Pt(II) centre in the tri-coordinated electrophilic species **7**[50] using local properties and natural charges (see the ESI).† Lower values are obtained for the attack involving N1 as donor in comparison to the case of attack through N7, for either $\Delta(s^2)_{kl}$ (0.07 and 0.38, respectively) and $\Delta(\omega^2)_{kl}$ (1.6×10^{-2} and 2.5×10^{-2}, respectively), thus pointing to a kinetically preferred binding of the 7-azaindolate ligand using its pyrrole-like N1 atom,[51] as experimentally observed.

Inclusion of a π-stacked Haza unit on the previously computed geometry **8** affords the structure $\mathbf{4}^{calcd}$ that nicely agrees with the experimentally obtained geometry for **4** (Table 1). Although small, the most significant discrepancies deal with a slight overestimation of the π-stacking of the free Haza unit in opening the C_6F_5–Pt–C_6F_5 angle and, obviously, with the H atom position in the N–H···N hydrogen bond. According to our calculations inclusion of the π-stacked Haza unit is expected to be only slightly favoured ($\Delta E = -1.02$ kcal mol^{-1}). Two sets of binding forces holding together both units operate in almost orthogonal directions and can be quantified separately. Parallel alignment of the aromatic Haza unit to one C_6F_5 ligand (C1–C6 fragment in Fig. 2) provides a first stabilization source through π,π-stacking interaction (WBI_{total} 0.060). It is characterized by two BCPs (bond critical points) within the framework of Bader's atoms-in-molecules (AIM) theory[52] ($\rho(\mathbf{r}_c)_{total} = 1.38 \times 10^{-2}$ e/a_o^3), exhibiting the typical large ε values of diagnostic relevance for these type of interactions ($\varepsilon_{aver} = 0.84$). On the other hand, two H atoms in Haza lie close enough to another almost orthogonal C_6F_5 ligand (C7–C12 fragment in Fig. 2), thus allowing formation of a comparatively weaker T-shaped H···π stacking interaction (WBI_{total} 0.037) for which only one BCP was found ($\rho(\mathbf{r}_c) = 6.28 \times 10^{-3}$ e/a_o^3; $\varepsilon = 0.22$).

Crystal structure of 6·$CHCl_3$

The structure of the diplatinate dianion in **6**·$CHCl_3$ is shown in Fig. 4. The core of the anion comprises two platinum atoms 3.177 Å apart, bridged by an OH and an aza ligands. The bridging azaindolate is disordered in an about 50 : 50 distribution. The platinum···platinum separation is shorter than the van der Waals radii sum, the metal···metal distance observed in the related dinuclear complex $[NBu_4][\{Pt(C_6F_5)_3\}_2(\mu\text{-OH})(\mu\text{-Pb})]$ being 3.494 Å.[53] The steric constraints imposed by the bridging ligands in the diplatinate complex of **6**·$CHCl_3$ also cause the coordination planes of the platinum atoms to form an angle of 78.11°. The platinum–N distances are in good agreement with the values found in compound **4**. An almost face-to-face (rather than the typical slipped) π-stacking interaction between two of the electron-poor C_6F_5 ligands is also observed (Fig. 4), showing a rather short centroid–centroid contact (Ct···Ct = 3.740(2) Å, interplanar angle 12.4(2)° and centroid-to-plane separation 3.72 Å).[30] C–H···F intermolecular interactions are present, with the three shortest hydrogen bonds being F19···H58B, F8···H59A, and F5···H57A (2.33, 2.41, and 2.44 Å, respectively). Other intermolecular interaction contacts observed are of the type C–H···π_{aza}.[33,36,37] Fluorine atoms of the C_6F_5 groups may function as intramolecular hydrogen-bond acceptors for the bridging OH group (H···F16 2.54(4), O1···F16

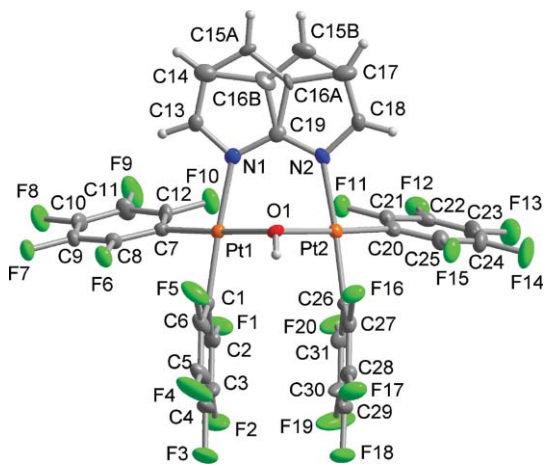

Fig. 4 ORTEP representation (50% probability) of the anion of **6**·$CHCl_3$. The disorder of the azaindolate ligand is explained in the text. See Table 2 for bond distances and angles.

Table 2 Selected bond lengths (Å) and angles (°) for **6**·$CHCl_3$ and $\mathbf{6}^{calcd\,a}$

	6·$CHCl_3$	$\mathbf{6}^{calcd\,a}$
Pt1–C1, Pt2–C26	2.005(4), 2.009(4)	2.017, 2.018
Pt1–C7, Pt2–C20	1.984(4), 1.989(4)	2.004, 2.000
Pt1–O1, Pt2–O1	2.094(3), 2.078(3)	2.117, 2.120
Pt1–N1, Pt2–N2	2.092(4), 2.072(3)	2.120, 2.104
Pt1–Pt2	3.1773(2)	3.247
F1 ··· F20	3.196	3.266
F10 ··· F11	3.542	3.598
C1–Pt1–C7, C26–Pt2–C20	90.69(15), 91.70(16)	90.94, 91.22
C1–Pt1–O1, C26–Pt2–O1	90.55(13), 90.22(13)	92.46, 91.65
C7–Pt1–N1, C20–Pt2–N2	92.97(13), 93.35(14)	91.73, 92.44
Pt1–O1–Pt2	99.19(11)	100.06

^{a} $\mathbf{6}^{calcd} = [Pt(C_6F_5)_2(\mu\text{-OH})(\mu\text{-aza-N7,N1})]^{2-}$.

3.016(3) Å, O1–H ··· F16 125(4)° and H ··· F5 2.58(4), O1 ··· F5 3.001(4), O1–H ··· F5 120(4)).

Compound **6**·$CHCl_3$ crystallizes in the non-centrosymmetric polar space group *Cc*. Accordingly, the molecules must show a polar packing by having the same orientation along the polar *c* axis: with their azaindolate ends, for example, the anions are all pointing in the same direction (along the vertical polar *c* axis in Fig. 5).

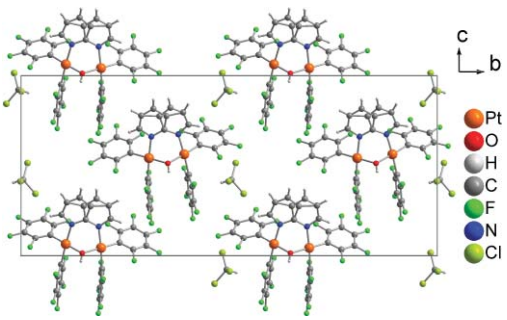

Fig. 5 Projection of the unit cell packing of the anion and chloroform solvate of **6**·$CHCl_3$ along *a* to illustrate the polar packing along the vertical polar *c* axis (ammonium cations and chloroform disorder have been removed for clarity).

Theoretical calculations on the dianion of compound 6

The calculated structure $\mathbf{6}^{calcd}$ = $[\{M(C_6F_5)_2\}_2(\mu\text{-OH})(\mu\text{-aza-N7,N1})]^{2-}$, although in very good general agreement with the experimental one, slightly underestimates the Pt ··· Pt interaction ($WBI_{Pt\cdots Pt}$ 0.038). Despite this obvious contact between the Pt atoms, below the sum of their van der Waals radii, no BCP was found. It could be tentatively interpreted in terms of a difficult topological analysis of the electronic charge density $\rho(\mathbf{r}_c)$ in the complex region situated among the two Pt atoms and the hydroxo ligand. Indeed the MO analysis reveals the existence of a HOMO with antibonding character with respect to the Pt ··· Pt interaction (Fig. 6),[54] as well as three other lower bonding combinations (HOMO-5, HOMO-6 and HOMO-8) and two very low lying HOMOs (*i.e.* HOMO-16 and HOMO-21) corresponding to bonding zero-nodal combinations of the three-centre two-electron interaction within a three-membered oxadiplatinirane ring (see the ESI).† Also no BCP was observed between the almost parallel C_6F_5 rings ($d_{Ct\cdots Ct}$ = 4.069 Å, sum of $WBI_{Ar\cdots Ar}$ 0.011).

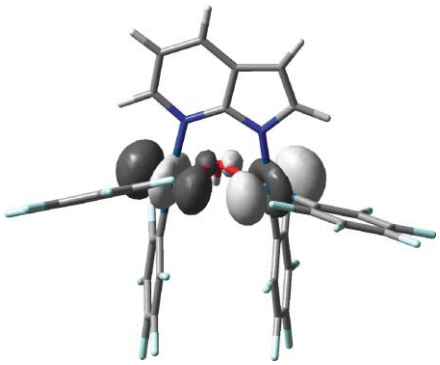

Fig. 6 Calculated HOMO surface (iso-value 0.04) for $\mathbf{6}^{calcd}$.

This optimized geometry for $\mathbf{6}^{calcd}$ also corroborates the *anti* orientation of the hydroxo H atom with respect to the bridging aza ligand. The OH ligand forms two moderately strong H ··· F hydrogen bonds with the nearest *ortho*-F atoms ($d_{H\cdots F}$ = 2.323 and 2.550 Å, WBI 0.008 and 0.003) with well defined BCP for the former ($\rho(\mathbf{r}_c) = 1.08 \times 10^{-2}$ e/a_o^3), as also observed in the X-ray structure (see above). This H–F hydrogen bonding establishes the difference with respect to the other possible conformer with *syn* hydroxo orientation, that is 2.62 kcal mol^{-1} less stable in the potential energy surface. It is worth to note that two *ortho*-F atoms belonging to the other C_6F_5 groups lie very close to each other ($d_{F\cdots F}$ = 3.267 Å, WBI 0.001, $\rho(\mathbf{r}_c) = 1.70 \times 10^{-3}$ e/a_o^3).

Neutral complexes [Pt(dmba)(aza-N1)(L)] [L = DMSO, PPh_3]

The platinum complexes [Pt(dmba)(aza-N1)(L)] [L = DMSO (**9**), PPh_3 (**10**)] have been prepared from the corresponding chloro platinum complex [Pt(dmba)(L)Cl] (L = DMSO or PPh_3)[55] (Scheme 4). After precipitation of AgCl by addition of $AgClO_4$ in a 1 : 1 molar ratio in acetone, the solvent complexes $[Pt(dmba)(L)(Me_2CO)]ClO_4$ generated *in situ* react with 1 equiv. of both 7-azaindole and KOH/MeOH to give the neutral complexes **9** and **10**. The structures were assigned also on the basis of microanalytical, and ^1H, ^{195}Pt and ^{31}P NMR data (for **10**). The ^1H NMR spectra of complexes **9** and **10** show that both the *N*-methyl groups and the methylene protons of the dmba are diastereotopic, two separate singlets being observed for the former and two close AB doublets for the later. Therefore, there is no plane of symmetry in the metal coordination plane. The ^1H resonances assigned to H2 of the aza ligand for **9** and **10** are flanked by ^{195}Pt satellites, which are also observed in several others resonances of complexes **9** and **10** (see the Experimental). In complex **10** the phosphine-*trans*-to-NMe_2 ligand arrangement in the starting material[55] is preserved, after chlorine abstraction and aza coordination, as can be inferred by ^1H NMR from the small, but significant, coupling constant

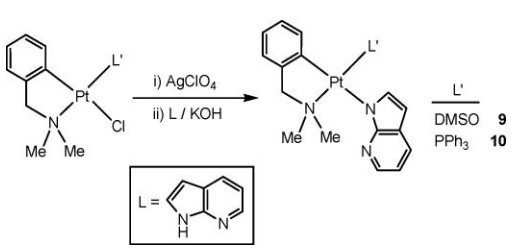

Scheme 4

$^4J_{P\text{-}H}$ (2.4–4.2 Hz) of the CH_2N or the NMe_2 protons of dmba with the phosphorus atom.

Compound **9** crystallizes with half a molecule of crystal water and a quarter molecule of toluene per molecular formula unit as **9**·0.5H_2O·0.25C_7H_8. The coordination at platinum in **9** is square-planar with the DMSO ligand *trans* to the dmba nitrogen atom (Fig. 7). The center of inversion in $P\bar{1}$ is occupied by the toluene solvent molecule which shows its typical disorder around an inversion center (ESI, Fig. S7).†

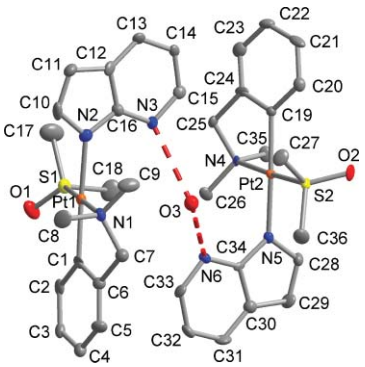

Fig. 7 ORTEP representation (50% probability) of the dimeric entity of **9**·0.5H_2O. The hydrogen atoms on O3 could not be found in this heavy atom structure. Distances and angles in Table 3; hydrogen bonding interaction as dashed line. Hydrogen atoms on carbon have been omitted for clarity.

The hydrogen-bonding action of the crystal water molecule to the pyridine N atoms joins two molecules of **9** into a dimer (Fig. 7) which then have to be symmetry independent (as the inversion center is already taken by the toluene solvent. Except for the solvent molecules this represents a $Z' = 2$ ($Z' > 1$) structure.[31,56–58]

Besides the noted hydrogen-bonding interactions, the packing in **9**·0.5H_2O·0.25C_7H_8 is solely controlled by C–H $\cdots$ π interactions; there is no π-stacking.[30,36]

Biological assays. Circular dichroism spectroscopy

The circular dichroism (CD) spectra of calf thymus DNA alone and incubated with the new platinum(II) compounds **4**, **9**, and **10** at 37 °C for 24 h with several molar ratios were recorded.

The changes in ellipticity and wavelength caused by compounds **9** and **10** are significant (Fig. 8). These results suggest modifications in the secondary structure of DNA caused by complexes **9** and **10**.[21–23,59–64] No important changes are observed for both the free Haza and complex **4**.

Gel electrophoresis of compound–pBR322 complexes

The influence of the compounds on the tertiary structure of DNA was determined by their ability to modify the electrophoretic mobility of the covalently closed circular (ccc) and open (oc) forms of pBR322 plasmid DNA. The complexes **4**, **9** and **10** were incubated at the molar ratio $r_i = 0.50$ with pBR322 plasmid DNA at 37 °C for 24 h. Representative gel obtained for the Pt complexes **4**, **9** and **10** are shown in Fig. 9. The behaviour of the gel electrophoretic mobility of both forms, ccc and oc, of pBR322 plasmid and DNA:cisplatin adducts is consistent with previous reports.[64] When the pBR322 was incubated with the platinum compound **10** (lane 5) a single footprinting for both forms, ccc

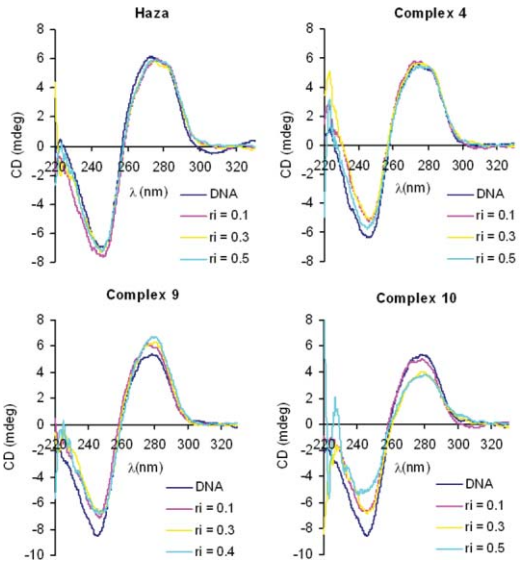

Fig. 8 Circular dichroism spectra of DNA and DNA incubated with complex **4**, complex **9** and complex **10** at different r_i.

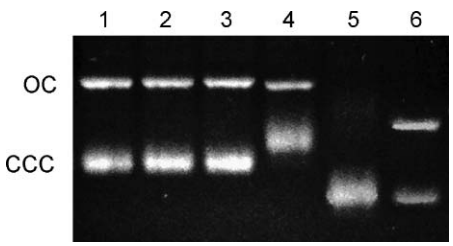

Fig. 9 Electrophoretic mobility pattern of pBR322 plasmid DNA incubated with Haza and their metal complexes: lane 1, pBR322; lane 2, Haza; lane 3, complex **4**; lane 4 complex **9**; lane 5, complex **10**; lane 6, CDDP.

and oc, coalescent form, was observed. A similar pattern has been found previously in some others dmba phosphine platinum complexes.[21,23] On the other hand, complex **9** (lane 4) delayed the mobility of the ccc form.

The behaviour observed for the electrophoretic mobility for the platinum complexes **9** and **10** indicates that some conformational changes occurred. This means that the degree of super helicity of the DNA molecules has been altered.

Cytotoxicity studies

To analyze the potential of the compounds as antitumour agents, their cytotoxicity was evaluated towards the human breast cancer (T47D, cisplatin resistant) and epithelial ovarian carcinoma cells A2780 and A2780*cis*R (acquired resistance to cisplatin) and for comparison purposes the cytotoxicity of cisplatin and the free ligands was evaluated under the same experimental conditions. Because of low aqueous solubility, the test compounds were dissolved in DMSO first and then serially diluted in complete culture medium such that the effective DMSO content did not exceed 1%.

The primary *in vitro* antitumour screening of complexes **2**, **4**, **6**, **9** and **10**, Cisplatin and the free ligands at 100 μM concentration (Table 4) shows that **4**, **9** and **10** exhibit activity in the low-micromolar range in all cell lines and values of IC_{50} were also

Table 3 Selected bond lengths (Å) and angles (°) for **9**·0.5H_2O·0.25C_7H_8[a]

	Pt1	Pt2
Pt–C(dmba)	2.013(10)	1.991(9)
Pt–N(dmba)	2.075(8)	2.060(8)
Pt–N(aza)	2.083(8)	2.084(7)
Pt–S	2.190(2)	2.185(2)
O3 ··· N(pyridine)	2.86(1)	2.80(1)
C–Pt–N(dmba)	81.8(4)	81.3(3)
C–Pt–N(pyridine)	172.0(3)	171.9(3)
N(dmba)–Pt–N(pyr)	90.2(3)	91.2(3)
C–Pt–S	95.9(3)	95.5(3)
N(dmba)–Pt–S	176.0(2)	176.4(2)
N(pyridine)–Pt–S	92.1(2)	92.2(2)
N3 ··· O3 ··· N6	121.4(3)	

[a] Two independent platinum molecules in the asymmetric unit.

Table 4 Percentage inhibition at 100 μM concentration for complexes **2**, **4**, **6**, **9** and **10**, cisplatin and the free ligands in the human breast and ovarian carcinoma cell lines T47D, A2780 and A2780*cis*R

Complex	T47D 48 h	A2780 48 h	A2780*cis*R 48 h
2	15 ± 4	48 ± 4	35 ± 5
4	70 ± 3	83 ± 1	89 ± 2
6	45 ± 3	80 ± 2	83 ± 3
9	78 ± 2	91 ± 1	85 ± 1
10	82 ± 1	91 ± 2	91 ± 2
Cisplatin	70 ± 3	91 ± 1	87 ± 2
PPh_3	38 ± 4	20 ± 5	13 ± 4
7-Azaindole	2 ± 1	3 ± 2	2 ± 1
Dmba	1 ± 1	2 ± 1	2 ± 2

Table 5 IC_{50} (μM) and resistance factors for cisplatin and complexes **5**, **9** and **10**

Complex	T47D 48 h	A2780 48 h	A2780*cis*R 48 h (*RF*)[a]
4	19 ± 3	5.8 ± 0.3	12 ± 2 (2.1)
9	0.53 ± 0.05	0.34 ± 0.02	0.45 ± 0.02 (1.3)
10	4.8 ± 0.1	2.7 ± 0.1	2.0 ± 0.04 (0.7)
Cisplatin	37 ± 4	0.87 ± 0.03	11 ± 3 (12.6)

[a] The numbers in parentheses are the resistance factors *RF* (IC_{50} resistant/IC_{50} sensitive).

calculated for them (Table 5). Noteworthy, at 48 h incubation time the platinum complex **4** shows sub-micromolar activity both in A2780 and T47D [IC_{50} (μM)= 0.34 and 0.53, respectively]. On the other hand, A2780*cis*R encompasses all of the known major mechanisms of resistance to cisplatin: reduced drug transport,[65] enhanced DNA repair/tolerance[66] and elevated GSH levels.[67] The ability of complexes **4**, **9** and **10** to circumvent cisplatin acquired resistance was determined from the resistance factor (*RF*), defined as the ratio of IC_{50} resistant line to IC_{50} parent line. An *RF* of <2 was considered to denote non-cross resistance.[68] Especially noteworthy are the very low resistance factors (*RF*) of these new complexes at 48 h (*RF* = 0.7–2.1) indicating efficient circumvention of cisplatin resistance (Table 5).

The stability of the cytotoxic compounds **4**, **9** and **10** have been studied in DMSO by ^{1}H NMR. Complexes **9** and **10** remained unaltered after six days in solution at room temperature, although H/D exchange was observed for the coordinated DMSO resonances of complex **9**. The stability of complex **4** in DMSO solution was smaller, some changes being observed after 10 h in solution.

Conclusions

A series of new 7-azaindolyl palladium and platinum complexes have been prepared. Among them we report the unprecedented cases of mixed azaindole–azaindolate metal complexes where two different binding modes of acid/base related ligands co-exist. The structures of $[NBu_4][M(C_6F_5)_2(Haza\text{-}N7)(aza\text{-}N1)]\cdot Haza$ (M = Pd, Pt) were isomorphous. Their X-ray structure determinations have established the existence of an intramolecular N–H ··· N contact between the two coordinated azaindolyl groups and intermolecular head-to-tail N–H ··· N contacts between the free 7-azaindole molecules. Theoretical calculations show that both kinetic and thermodynamical arguments support the observed coordination and H-bonding interaction of the pyrrolo and the pyridine moieties of the neutral and deprotonated heterociclic ligands. At 48 h incubation time the new platinum complex **9** shows sub-micromolar activity both in A2780 and T47D [IC_{50} (μM) = 0.34 and 0.53, respectively], and also very low resistance factors against an A2780 cell line which has acquired resistance to cisplatin (*RF* = 1.3). The DNA adduct formation of the new platinum complexes **9** and **10** was followed by circular dichroism suggesting modifications in the secondary structure of DNA. The behaviour observed for the electrophoretic mobility for **9** and **10** indicates alteration of the degree of super helicity of the DNA molecules.

Experimental

Instrumental measurements

The CHNS analyses were performed with a Carlo Erba model EA 1108 microanalyzer. Decomposition temperatures were determined with a SDT 2960 simultaneous DSC-TGA of TA instruments at a heating rate of 5 °C min^{-1} and the solid samples under nitrogen flow (100 mL min^{-1}). The ^{1}H, ^{19}F and ^{195}Pt NMR spectra were recorded on a Bruker AC 300E, Bruker AC 400E or Bruker AV 600 spectrometer, using $SiMe_4$, H_3PO_4, $CFCl_3$ and $Na_2[PtCl_6]$ as standards. Infrared spectra were recorded on a Perkin-Elmer 1430 spectrophotometer using Nujol mulls between polyethylene sheets. Mass spectra (positive-ion FAB) were recorded on a V. G. AutoSpecE spectrometer and measured using 3-nitrobenzyl alcohol as the dispersing matrix.

Materials

The starting complexes $[M(C_6F_5)_2(NCPh)_2]$ (M = Pd, Pt),[17,18] $[NBu_4]_2[M(C_6F_5)_2(\mu\text{-}OH)]_2$ (M = Pd, Pt)[18,26] and [Pt(dmba)(L)Cl] (L = DMSO or PPh_3)[55] were prepared by procedures described elsewhere. Solvents were dried by the usual methods.

Preparation of [*cis*-bis(7-azaindole-κN7)bis(pentafluorophenyl)-metall(II)] complexes, $[M(C_6F_5)_2(Haza)_2]$ [M = Pd (1), Pt (2)]

To a solution of $[M(C_6F_5)_2(NCPh)_2]$ (0.155 mmol) in CH_2Cl_2 (15 mL) 7-azaindole (36.62 mg, 0.310 mmol) was added. The resulting mixture was stirred at room temperature for 1 h, and then the solvent was partially evaporated under vacuum and hexane

added to precipitate a white solid, which was collected by filtration and air-dried. **1**: Yield: 74 mg (71%). Calcd for $C_{26}H_{12}F_{10}N_4Pd$: C 46.14, H 1.79, N 8.28. Found: C 46.12, H, 1.65, N 8.26. Mp: 258 °C (decomposition). IR (Nujol, cm^{-1}): 3444 ν(N–H), 800, 784 ν(Pd–C_6F_5). ^{1}H NMR ($CDCl_3$): δ 9.77 (br, 2 H, NH, Haza), 8.19 (dd, 2 H, H6, Haza, J(HH) = 5.4 Hz, J(HH) = 1.2 Hz), 7.86 (d, 2 H, H4, Haza, J(HH) = 7.8), 7.43 (dd, 2 H, H2, Haza, J(HH) = 3.6 Hz, J(HH) = 2.7 Hz), 6.92 (dd, 2 H, H5, Haza, J(HH) = 7.8 Hz, J(HH) = 5.4 Hz), 6.51 (dd, 2 H, H3, Haza, J(HH) = 3.6 Hz, J(HH) = 2.1 Hz). ^{19}F NMR ($CDCl_3$): δ –116.7 (m, 4 F_o), –160.1 (t, 2 F_p, $J(F_pF_m)$ = 19.7 Hz), –162.5 (m, 4 F_m). **2**: Yield: 79 mg (77%). Calcd for $C_{26}H_{12}F_{10}N_4Pt$: C 40.80, H 1.58, N 7.32. Found: C 40.68, H 1.59, N 7.21. Mp: 311 °C (decomposition). IR (Nujol, cm^{-1}): 3434 ν(N–H), 812 ν(Pt–C_6F_5), 800. ^{1}H NMR ($CDCl_3$): δ 10.01 (br, 2 H, NH, Haza), 8.30 (dd, 2 H, H6, Haza, J(HH) = 5.2 Hz, J(HH) = 0.8 Hz, Pt satellites are observed as shoulders), 7.89 (d, 1 H, H4, Haza, J(HH) = 7.6 Hz), 7.45 (dd, 1 H, H2, Haza, J(HH) = 3.6 Hz, J(HH) = 2.8 Hz), 6.95 (dd, 1 H, H5, Haza, J(HH) = 7.6 Hz, J_{HH} = 5.2 Hz), 6.56 (dd, 1 H, H3, Haza, J_{HH} = 3.6 Hz, J_{HH} = 2.0 Hz). ^{19}F NMR ($CDCl_3$): δ –120.3 (m, 4 F_o, J(PtF_o) = 492.7 Hz), –161.6 (t, 2 F_p, $J(F_pF_m)$ = 19.7 Hz), –163.7 (m, 4 F_m). ^{195}Pt NMR ($CDCl_3$): δ –3625 (m).

Preparation of (tetra-*n*-butylammonium)[*cis*-(7-azaindolato-κN1)-(7-azaindole-κN7)bis(pentafluorophenyl)metallate(II)]·7-azaindole complexes, [NBu_4][Pt(C_6F_5)$_2$(Haza)(aza)]·Haza [M = Pd (3), Pt (4)]

To a solution of [M(C_6F_5)$_2$(Haza)$_2$] (0.148 mmol) in acetone (15 mL) 7-azaindole (17.48 mg, 0.148 mmol) and finally 20% [NBu_4]OH (aq) (194 μL, 0.148 mmol) were added. The mixture was stirred at room temperature for 20 h and then solvent was evaporated to dryness. The residue was treated with Et_2O to give a white solid, which was collected by filtration and air-dried.

Alternative method of preparation of complex 3. To a solution of [NBu_4]$_2$[Pd(C_6F_5)$_2$(μ-OH)]$_2$ (100 mg, 0.071 mmol) in CH_2Cl_2 (15 mL) was added 7-azaindole (67.5 mg, 0.571 mmol). The resulting mixture was stirred for 20 h at room temperature and then solvent was evaporated to dryness. The residue was treated with Et_2O to give a white solid, which was collected by filtration and air-dried.

3: Yield: 120 mg (78%), (112 mg, 75% for alternative method). Calcd for $C_{49}H_{53}F_{10}N_7Pd$: C 56.79, H 5.15, N 9.46. Found: C 56.48, H 5.30, N 9.49. Mp: 174 °C (decomposition). IR (Nujol, cm^{-1}): 802, 792 ν(Pd–C_6F_5). ^{1}H NMR (CD_2Cl_2): δ 8.44 (dd, 1 H, H6, Haza, J(HH) = 5.4 Hz, J(HH) = 1.4 Hz), 8.33 (m, 2 H, H6, aza + H6 of free Haza), 7.99 (dd, 1 H, H4, aza or free Haza, J(HH) = 7.8 Hz, J(HH) = 1.4 Hz), 7.82 (dd, 1 H, H4, Haza, J(HH) = 7.8 Hz, J_{HH} = 1.4 Hz), 7.66 (m, 2 H, H2 of aza + H4 of aza or free Haza), 7.41 (m, 2 H, H2, Haza + H2, free Haza), 7.11 (dd, 1 H, H5, aza or free Haza, J(HH) = 7.8 Hz, J(HH) = 4.8 Hz), 6.88 (dd, 1 H, H5, Haza, J(HH) = 7.8 Hz, J(HH) = 5.4 Hz), 6.74 (dd, 1 H, H5, aza or free Haza, J(HH) = 7.6 Hz, J(HH) = 4.6 Hz), 6.54 (d, 1 H, H3, Haza or free Haza, J(HH) = 3.6), 6.39 (d, 1 H, H3, Haza or free Haza, J_{HH} = 3.6), 6.22 (d, 1 H, H3, aza, J(HH) = 2.8). ^{19}F NMR ($CDCl_3$): δ –114.8 (m, 2 F_o), –115.6 (m, 2 F_o), –164.3 (t, 1 F_p, $J(F_pF_m)$ = 20.7 Hz), –164.9 (t, 1 F_p, $J(F_pF_m)$ = 20.7 Hz), –165.2 (m, 2 F_m), –165.8 (m, 2 F_m). **4**: Yield: 114 mg (68%). Calcd for $C_{49}H_{53}F_{10}N_7Pt$: C 52.31, H 4.75, N 8.71. Found: C 52.07, H 5.01, N 8.53. Mp: 211 °C (decomposition). IR (Nujol, cm^{-1}): 802, 792 ν(Pt–C_6F_5). ^{1}H NMR (CD_2Cl_2): δ 8.46 (dd, 1 H, H6, aza a, J(HH) = 5.4 Hz, J(HH) = 0.8 Hz, Pt satellites are observed as shoulders), 8.28 (m, 2 H, H6, Haza + H6 free Haza), 7.95 (dd, 1 H, H4, aza or free Haza, J(HH) = 7.8 Hz, J(HH) = 1.4 Hz), 7.80 (dd, 1 H, H4, Haza, J(HH) = 7.8 Hz, J(HH) = 1.0 Hz), 7.63 (m, 2 H, H2 of aza + H4 of aza or free Haza, satellites are observed as shoulders), 7.36 (m, 2 H, H2, Haza + H2, free Haza), 7.08 (dd, 1 H, H5, aza or free Haza, J_{HH} = 8.0 Hz, J(HH) = 4.8 Hz), 6.83 (dd, 1 H, H5, Haza, J(HH) = 7.6 Hz, J(HH) = 5.4 Hz), 6.70 (dd, 1 H, H5, aza or free Haza, J_{HH} = 7.6 Hz, J(HH) = 4.8 Hz), 6.51 (d, 1 H, H3, Haza or free Haza, J(HH) = 3.6 Hz), 6.38 (d, 1 H, H3, Haza or free Haza, J(HH) = 3.4), 6.16 (d, 1 H, H3, aza, J(HH) = 2.8). ^{19}F NMR (CD_2Cl_2): δ –117.1 (m, 2 F_o, J(PtF_o) = 546.2 Hz), –119.6 (m, 2 F_o, J(PtF_o) = 498.8 Hz), –166.6 (m, 2 F_p + 4 F_m). ^{195}Pt NMR (CD_2Cl_2): δ –3495 (m).

Preparation of bis(tetra-*n*-butylammonium)-[*cis*(μ-7-azaindolato-κN1:N7)(μ-hydroxo)-tetrakis(pentafluorophenyl)dipalladate(II)], [NBu_4]$_2$[{Pd(C_6F_5)$_2$}$_2$(μ-OH)(μ-aza)] (5)

To a solution of [NBu_4]$_2$[Pd(C_6F_5)$_2$(μ-OH)]$_2$ (100 mg, 0.071 mmol) in CH_2Cl_2 (15 mL) was added 7-azaindole (8.4 mg, 0.071 mmol). The resulting solution was stirred at room temperature for 1 h, and then the solvent was partially evaporated under vacuum and hexane added to precipitate a white solid, which was collected by filtration and air-dried. **5**: Yield: 87 mg (81%). Calcd for $C_{63}H_{78}F_{20}N_4OPd_2$: C 50.44, H 5.24, N 3.73. Found: C 50.12; H 5.45, N 3.78. Mp: 213 °C (decomposition). IR (Nujol, cm^{-1}): 3606 ν(O–H), 792, 778 ν(Pd–C_6F_5). ^{1}H NMR ($CDCl_3$): δ 7.65 (dd, 1 H, H4, aza, J(HH) = 7.5 Hz, J(HH) = 1.2 Hz), 7.45 (d, 1 H, H6, aza, J(HH) = 5.4 Hz), 6.84 (d, 1 H, H2, aza, J_{HH} = 2.4 Hz), 6.47 (dd, 1 H, H5, aza, J(HH) = 7.5 Hz, J(HH) = 5.4 Hz), 6.15 (d, 1 H, H3, aza, J(HH) = 2.7 Hz), –1.34 (s, 1 H, OH). ^{19}F NMR ($CDCl_3$): δ –112.7 (m, 2 F_o), –113.2 (m, 2 F_o), –113.4 (m, 2 F_o), –113.8 (m, 2 F_o), –163.8 (t, 1 F_p, $J(F_pF_m)$ = 19.7 Hz), –164.1 (t, 1 F_p, $J(F_pF_m)$ = 19.7 Hz), –164.5 (t, 1 F_p, $J(F_pF_m)$ = 19.7 Hz), –165.3 (t, 1 F_p, $J(F_pF_m)$ = 19.7 Hz), –165.6 (m, 6 F_m), –166.1 (m, 2 F_m).

Preparation of bis(tetra-*n*-butylammonium)-[*cis*(μ-7-azaindolato-κN1:N7)(μ-hydroxo)-tetrakis(pentafluorophenyl)diplatinate(II)], [NBu_4]$_2$[{Pt(C_6F_5)$_2$}$_2$(μ-OH)(μ-aza)] (6)

To a suspension of [NBu_4]$_2$[Pt(C_6F_5)$_2$(μ-OH)]$_2$ (100 mg, 0.063 mmol) in toluene (15 mL) was added 7-azaindole (15.0 mg, 0.126 mmol). The resulting mixture was stirred under reflux for 7 h, filtered through a short pad of Celite and then the solvent was evaporated to dryness. The residue was treated with Et_2O to give a white solid, which was collected by filtration and air-dried. **6**: Yield: 75 mg (70%). Calcd for $C_{63}H_{78}F_{20}N_4OPt_2$: C 45.11, H 4.69, N 3.34. Found: C 44.82, H 4.81, N 3.45. Mp: 261 °C (decomposition). IR (Nujol, cm^{-1}): ν(O–H) 3606, ν(Pt–C_6F_5) 808, 798. ^{1}H NMR ($CDCl_3$): δ 7.76 (dd, 1 H, H4, aza, J(HH) = 7.5 Hz, J(HH) = 1.2 Hz), 7.60 (dd, 1 H, H6, aza, J(HH) = 5.4 Hz, J(HH) = 1.2 Hz, Pt satellites are observed as shoulders), 6.93 (d, 1 H, H2, aza, J(HH) = 2.7 Hz, Pt satellites are observed as shoulders), 6.46 (dd, 1 H, H5, aza, J(HH) = 7.5 Hz, J(HH) = 5.4 Hz), 6.21 (d, 1 H, H3, aza, J(HH) = 2.7 Hz), –0.12 (s, 1 H, OH). ^{19}F NMR ($CDCl_3$):

δ –117.4 (m, 4 F_o), –118.3 (m, 2 F_o), –119.1 (m, 2 F_o), –165.6 (t, 1 F_p, $J(F_pF_m)$ = 19.7 Hz), –166.1 (t, 1 F_p, $J(F_pF_m)$ = 19.7 Hz), –166.9 (m, 1 F_p + 6 F_m), –167.7 (m, 2 F_m), –166.1 (m, 2 F_m). ^{195}Pt NMR ($CDCl_3$): δ –3147 (m), –3190 (m).

Preparation of (7-azaindolato-κN1)(*N*,*N*-dimethylbenzylamine-κN,κC)-(dimethylsulfoxide-κS)/(triphenylphosphane)-palladium(II) [Pt(dmba)(aza-N1)(L)] [L = DMSO (9), PPh_3 (10)]

To a solution of [Pt(dmba)(Cl)(L)] (L = DMSO, PPh_3) (0.24 mmol) in acetone (20 mL) $AgClO_4$ (0.24 mmol) was added. AgCl immediately formed. The resulting suspension was stirred for 30 min in the darkness and then filtered through a short pad of Celite. The filtrate was then evaporated to dryness and the residue treated with a mixture of 7-azaindole (0.24 mmol) and KOH (0.96 mmol) in methanol (20 mL). The mixture was stirred at room temperature for 1 h and then evaporated to dryness. The residue was treated with CH_2Cl_2 (20 mL) and filtered through a short pad of Celite. The resulting solution was partially evaporated under vacuum and hexane added to precipitate a white solid, which was collected by filtration and air-dried. **9**: Yield: 130 mg (73%). Calcd for $C_{18}H_{23}N_3OSPt$: C 41.22, H 4.42, N 8.01, S 6.11. Found: C 41.09, H 4.51, N 7.98, S 6.08. Mp: 183 °C (decomposition). ^{1}H NMR ($CDCl_3$): δ($SiMe_4$) 8.22 (dd, 1 H, H6, aza, J(HH) = 4.8 Hz, J(HH) = 1.5 Hz), 7.96 (m, 1 H, aromatic of dmba, Pt satellites are observed as shoulders), 7.88 (dd, 1 H, H4, aza, J(HH) = 7.8 Hz, J(HH) = 1.5 Hz), 7.38 (d, 1 H, H2, aza, J(HH) = 2.9 Hz, satellites are observed as shoulders), 7.08 (m, 3 H, aromatics of dmba), 6.85 (dd, 1 H, H5, aza, J(HH) = 7.8 Hz, J(HH) = 4.8 Hz), 6.51 (d, 1 H, H3, aza, J(HH) = 2.9 Hz), 4.26 (d, 1 H, CH_2N, J(HH) = 13.5 Hz, J(HPt) = 25.5 Hz), 3.84 (d, 1 H, CH_2N, J(HH) = 13.5 Hz, J(HPt) = 56.7 Hz), 3.39 (s, 3 H, DMSO, J(HPt) = 30.3 Hz), 2.57 (s, 3 H, N(CH_3)$_2$, J(HPt) = 37.2 Hz), 2.53 (s, 3 H, DMSO, J(HPt) = 19.2 Hz), 2.33 (s, 3 H, N(CH_3)$_2$, J(HPt) = 35.1 Hz). ^{195}Pt NMR ($CDCl_3$): δ($Na_2[PtCl_6]$) –3645 (s). **10**: Yield: 150 mg (83%). Calcd for $C_{34}H_{32}N_3PPt$: C 57.62, H 4.55, N 5.93. Found: C 57.34, H 4.43, N 5.65. Mp: 298 °C (decomposition). ^{1}H NMR ($CDCl_3$): δ($SiMe_4$) 7.98 (dd, 1 H, H6, aza, J(HH) = 4.4 Hz, J(HH) = 1.6 Hz), 7.57 (m, 6 H, PPh_3), 7.51 (dd, 1 H, H4, aza, J(HH) = 7.6 Hz, J(HH) = 1.6 Hz), 7.22 (m, 3 H, PPh_3), 7.10 (m, 6 H, PPh_3 + 1 H, aromatic of dmba), 6.99 (d, 1 H, H2, aza, J(HH) = 2.8 Hz, Pt satellites are observed as shoulders), 6.87 (vtd, 1 H, aromatic of dmba, J(HH) = 8.0 Hz, J(HP) = 0.8 Hz), 6.58 (m, 2 H, H5 of aza + H of aromatic of dmba, Pt satellites are observed as shoulders), 6.43 (vtd, 1 H, aromatic of dmba, J(HH) = 8.0 Hz, J(HP) = 0.8 Hz), 6.03 (d, 1 H, H3, aza, J(HH) = 2.8 Hz), 4.43 (d, 1 H, CH_2N, J(HH) = 13.2 Hz, Pt satellites are observed as shoulders), 3.89 (dd, 1 H, CH_2N, J(HH) = 13.2 Hz, J(HP) = 4.0 Hz, Pt satellites are observed as shoulders), 2.64 (d, 3 H, N(CH_3)$_2$, J(HP) = 2.4 Hz, J(HPt) = 28.5 Hz), 2.51 (d, 3 H, N(CH_3)$_2$, J(HP) = 3.2 Hz, J(HPt) = 24.3 Hz). ^{31}P NMR ($CDCl_3$): δ(H_3PO_4) 20.7 (s, J(PtP) = 4286 Hz). ^{195}Pt NMR ($CDCl_3$): δ($Na_2[PtCl_6]$) –3969 (d, J(PtP) = 4286 Hz).

X-Ray crystal structure analysis

Suitable crystals from **3** and **4** were grown from dichloromethane–toluene–hexane. Crystals of **6**·$CHCl_3$ were grown from $CHCl_3$, those of **9**·0.5H_2O·0.25C_7H_8 from CH_2Cl_2–toluene–hexane. The crystal and molecular structures of the compounds **3**, **4**, **6**·$CHCl_3$ and **9**·0.5H_2O·0.25C_7H_8 have been determined by X-ray diffraction studies (Table 6). The crystals were measured on a Bruker Smart Apex diffractometer. Data were collected using monochromated Mo Kα radiation in ω scan mode. Absorption corrections were applied on the basis of multi-scans. All structures were solved by direct methods using SHELX-97[69] and refined anisotropically on F^2. The NH hydrogen atoms were found and refined with U_{iso}(H) = 1.2U_{eq}(N). Hydrogen atoms for aromatic CH, aliphatic CH, CH_2 and methyl groups were positioned geometrically (C–H = 0.94 Å for aromatic CH, C–H = 0.99 Å for aliphatic CH, C–H = 0.98 Å for CH_2, C–H = 0.97 Å for CH_3) and refined using a riding model (AFIX 43 for aromatic CH, AFIX 13 for aliphatic CH, AFIX 23 for CH_2, AFIX 137 for CH_3), with U_{iso}(H) = 1.2U_{eq}(CH, CH_2) and U_{iso}(H) = 1.5U_{eq}(CH_3). For compound **6**·$CHCl_3$ the hydrogen atom on OH was found and refined with U_{iso}(H) = 1.5U_{eq}(O). The azaindolate is disordered in a 55 : 45 for A:B distribution. The chloroform crystal solvent is disordered over various positions. More than two different $CHCl_3$ positions are superimposed in the structure of **6**·$CHCl_3$ to give a variation in occupancies of different chlorine atoms. Significant residual electron densities in the near vicinity were added to the chloroform solvent. The disorder of the chloroform solvent cannot be satisfactorily solved, probably because of high mobility concomitant with little constraining van der Waals interactions. Thus, the chloroform atom positions should not be taken for any structure discussions but are solely meant to include and add the electron densities in a solvent accessible volume occupied by one highly disordered $CHCl_3$ molecule. In total there is one $CHCl_3$ molecule per asymmetric unit. In **6**·$CHCl_3$ the twelve strongest residual electron density peaks in the Fourier map are within 1.0 Å of either Pt1 or Pt2. In the structure of **9**·0.5H_2O·0.25C_7H_8 atoms C7 and C19 had to be refined isotropically because of non-positive definite or very oblate character despite attempted DELU restraints which were also applied to C1. The large residual electron density is within 1.0 Å of the Pt1 atom.

Graphics of the X-ray diffraction determined structures were drawn with DIAMOND (version 3.1f).[71] Computations on the supramolecular interactions were carried out with PLATON for Windows.[72] π-Stacking interactions can be viewed as medium to weak if they exhibit rather long centroid-centroid distances (Ct···Ct > 4.0 Å) together with large slip angles (β, γ > 30°) and vertical displacements (d > 2.0 Å). In comparison, strong π-stacking show rather short centroid-centroid contacts (< 3.8 Å), small slip angles (β, γ < 25°) and vertical displacements (d < 1.5 Å) which translate into a sizable overlap of the aromatic planes.[30,73]

Computational details

The reliably accurate description of weak interactions like those between ligands and heavy metals generally requires a treatment of electron correlation. Density functional theory (DFT)[74] has proved quite useful in this regard offering an electron correlation correction frequently comparable to the second-order Møller–Plesset theory (MP2) or in certain cases, and for certain purposes, even superior to MP2, but at considerably lower computational cost.[75] Calculated geometries at the DFT level were fully optimized in the gas-phase with tight convergence criteria using the Gaussian

Table 6 Crystal structure determination details

Compound	**3**	**4**	**6**·$CHCl_3$	**9**·$0.5H_2O$·$0.25C_7H_8$[d]
Empirical formula	$C_{49}H_{53}F_{10}N_7Pd$	$C_{49}H_{53}F_{10}N_7Pt$	$C_{64}H_{79}Cl_3F_{20}N_4OPt_2$	$C_{39.5}H_{52}N_6O_3Pt_2S_2$[e]
FW/g mol^{-1}	1036.38	1125.07	1796.84	1113.17
Crystal system	Monoclinic	Monoclinic	Monoclinic	Triclinic
a/Å	11.0967(5)	11.0665(5)	11.3030(5)	8.6147(15)
b/Å	18.6148(8)	18.6258(8)	37.3427(17)	10.4165(18)
c/Å	22.5261(10)	22.6090(10)	16.9524(8)	21.917(4)
α/°	90	90	90	84.523(2)
β/°	93.2170(10)	93.0130(10)	107.53(10)	87.574(2)
γ/°	90	90	90	82.352(2)
V/Å^3	4645.7(4)	4653.8(4)	6823(5)	1939.5(6)
T/K	100(2)	100(2)	100(2)	100(2)
Space group	$P2_1/c$	$P2_1/c$	Cc	$P\bar{1}$
Z	4	4	4	2[e]
D_c/Mg m^{-3}	1.482	1.606	1.749	1.906
μ/mm^{-1}	0.483	3.098	4.312	7.359
$F(000)$	2128	2256	3544	1086
Crystal size/mm	$0.40 \times 0.29 \times 0.17$	$0.27 \times 0.20 \times 0.13$	$0.21 \times 0.13 \times 0.08$	$0.20 \times 0.08 \times 0.05$
2θ range/°	3.62-56.56	3.60-56.46	3.94-54.70	3.74-50.10
h, k, l (range)	$-14 \le h \le 14$ $-23 \le k \le 23$ $-29 \le l \le 28$	$-12 \le h \le 14$ $-23 \le k \le 23$ $-28 \le l \le 28$	$-14 \le h \le 14$ $-48 \le k \le 47$ $-21 \le l \le 21$	$-10 \le h \le 10$ $-12 \le k \le 12$ $-26 \le l \le 26$
Max./min. transmission	0.9224/0.8303	0.6888/0.4884	0.7242/0.4645	0.7098/0.3207
Reflections collected (R_{int})	53617 (0.0257)	28314 (0.0251)	38715 (0.0257)	19493 (0.0373)
Independent reflections	10 811	10 375	14 964	6840
Observed reflections [$I > 2\sigma(I)$]	10 522	9241	14 488	6373
Restraints/parameters	0/614	1/614	3/895	2/469
Goodness-of-fit on F^2[a]	1.233	1.056	0.894	1.230
R_1, wR_2 [$I > 2\sigma(I)$][b]	0.0369/0.0827	0.0236/0.0583	0.0226/0.0470	0.0512/0.0955
R_1, wR_2 (all reflections)[b]	0.383/0.0835	0.0279/0.0600	0.0239/0.0474	0.0559/0.0971
Max./min. $\Delta\rho$/e Å^{-3}[c]	0.583/–0.472	1.232/–0.479	1.234/–0.520	4.843/–2.996
Absolute structure parameter (Flack value)[70]	—	—	0.008(3)	—

[a] Goodness-of-fit = $[\sum[w(F_o^2 - F_c^2)^2]/(n-p)]^{1/2}$. [b] $R_1 = \sum \|F_o\| - |F_c\| / \sum |F_o|$, $wR_2 = [\sum[w(F_o^2 - F_c^2)^2] / \sum w(F_o^2)^2]^{1/2}$; $w = 1/[\sigma^2(F_o^2) + (aP)^2 + bP]$, where $P = (2F_c^2 + F_o^2)/3$ and a and b are constants set by the program. [c] Largest difference peak and hole. [d] Two symmetry independent platinum molecules in the asymmetric unit; H atoms on the water of crystallization could not be found but were included in the empirical formula, calculation of the molecular mass, density and $F(000)$. [e] Checkcif suggests the doubled empirical formula with $Z = 1$.

03 package,[76] and employing the Truhlar's hybrid *meta* functional mPW1B95[77] that has been recommended for general purpose applications and was developed in order to produce a better performance where weak interactions are involved such as those between ligands and heavy metals.[78] The 6-31G** basis set was used in the optimizations for all atoms and adding diffuse functions on N and O atoms (denoted as aug6-31G**), as well as the Stuttgart relativistic small-core basis set with effective core potential (StRSCecp), for Pt. Ultrafine grids (99 radial shells and 590 angular points per shell) were employed for numerical integrations. From these gas-phase optimized geometries all reported data were obtained by means of single-point (SP) calculations at the same level. Energy values are uncorrected for the zero-point vibrational energy. Interaction energies were computed after correcting the basis set superposition error (BSSE) by means of the Bq method. Natural charges were obtained from the Natural Bond Orbital (NBO) population analysis. Bond orders were characterized by the Wiberg's bond index (WBI)[79] and calculated with the NBO method as the sum of squares of the off-diagonal density matrix elements between atoms. The topological analysis of the electronic charge density was conducted by means of the Bader's AIM methodology using the AIM2000 software.[80]

Biological assays. Circular dichroism study

Spectra were recorded at room temperature on an Applied Photophysics Π*-180 spectrometer with a 75 W xenon lamp using a computer for spectral subtraction and smooth reduction. The platinum samples ($ri = 0.1, 0.3, 0.5$) were prepared by addition of aliquots of each compound, from stock solutions (1 mg mL^{-1}), to a solution of calf thymus DNA (Sigma) in TE buffer (20 μg mL^{-1}), and incubated for 24 h at 37 °C. As a blank, a solution of each compound in TE buffer (50 mM NaCl, 10 mM Tris-HCl, 0.1 mM EDTA, pH 7.4) was used. Each sample was scanned twice in a range of wavelengths between 220 and 330 nm. The drawn CD spectra are the means of two independent scans. The ellipticity values are given in millidegrees (mdeg).

Electrophoretic mobility study

pBR322 plasmid DNA of 0.25 μg/μL concentration was used for the experiments. Four microlitres of charge maker (Lambda–pUC Mix Marker, 4) were added to aliquot parts of 20 μL of the drug–DNA complex. The platinum complexes were incubated at the molar ratio $r_i = 0.50$ with pBR322 plasmid DNA at 37 °C for

24 h. The mixtures underwent electrophoresis in agarose gel 1% in 1 × TBE buffer (45 mM Tris-borate, 1 mM EDTA, pH 8.0) for 5 h at 30 V. Gel was subsequently stained in the same buffer containing ethidium bromide (1 μg mL^{-1}) for 20 min. The DNA bands were visualized with a The DNA bands were visualized with an AlphaImager EC (Alpha Innotech).

Cell line and culture

The T-47D human mammary adenocarcinoma cell line used in this study was grown in RPMI-1640 medium supplemented with 10% (v/v) fetal bovine serum (FBS) and 0.2 unit/mL bovine insulin in an atmosphere of 5% CO_2 at 37 °C. The human ovarian carcinoma cell lines (A2780 and A2780*cis*R) used in this study were grown in RPMI 1640 medium supplemented with 10% (v/v) fetal bovine serum (FBS) and 2 mM L-glutamine in an atmosphere of 5% CO_2 at 37 °C.

Cytotoxicity assay

Cell proliferation was evaluated by assay of crystal violet. T-47D cells plated in 96-well sterile plates at a density of 5 × 103 cells per well with 100 μL of medium and were then incubated for 48 h. After attachment to the culture surface the cells were incubated with various concentrations of the compounds tested freshly dissolved in DMSO and diluted in the culture medium (DMSO final concentration 1%) for 48 h at 37 °C. The cells were fixed by adding 10 μL of 11% glutaraldehyde. The plates were stirred for 15 min at room temperature and then washed three to four times with distilled water. The cells were stained with 100 μL of 1% crystal violet. The plate was stirred for 15 min and then washed three to four times with distilled water and dried. One hundred microlitres of 10% acetic acid were added, and it was stirred for 15 min at room temperature. Absorbance was measured at 595 nm in a Tecan Ultra Evolution spectrophotometer.

The effects of complexes were expressed as corrected percentage inhibition values according to the following equation:

$$(\%)\ \text{inhibition} = [1 - (T/C)] \times 100 \quad (1)$$

where T is the mean absorbance of the treated cells and C the mean absorbance in the controls.

The inhibitory potential of compounds was measured by calculating concentration-percentage inhibition curves, and these curves were adjusted to the following equation:

$$E = E_{max}/[1 + (IC_{50})/C)^n] \quad (2)$$

where E is the percentage inhibition observed, E_{max} is the maximal effects, IC_{50} is the concentration that inhibits 50% of maximal growth, C is the concentration of compounds tested, and n is the slope of the semi-logarithmic dose-response sigmoidal curves. This non-linear fitting was performed using GraphPad Prism 2.01, 1996 software (GraphPad Software Inc.).

For comparison purposes, the cytotoxicity of cisplatin was evaluated under the same experimental conditions. All compounds were tested in two independent studies with triplicate points. The *in vitro* studies were performed in the USEF platform of the University of Santiago de Compostela (Spain).

Acknowledgements

This work was supported by the Ministerio de Educacion y Ciencia of Spain and FEDER (project CTQ2008-02178/BQU) and Fundacion Seneca-CARM (project 08666/PI/08). A. E. wants to acknowledge the financial support from MICINN-Spain, project CTQ2008-01402 and Fundación Séneca-CARM (project 04509/GERM/06).

Notes and references

1 G. La Monica and G. A. Ardizzoia, *Prog. Inorg. Chem.*, 1997, **46**, 151.
2 M. Fujita, *Chem. Soc. Rev.*, 1998, **27**, 417–425.
3 D. J. L. Tranchemontagne, Z. Ni, M. O'Keeffe and O. M. Yaghi, *Angew. Chem., Int. Ed.*, 2008, **47**, 5136–5147.
4 Y. Yamauchi, M. Yoshizawa and M. Fujita, *J. Am. Chem. Soc.*, 2008, **130**, 5832–5833.
5 E. C. Constable, *Coord. Chem. Rev.*, 2008, **252**, 842–855.
6 M. W. Cooke, D. Chartrand and G. S. Hanan, *Coord. Chem. Rev.*, 2008, **252**, 903–921.
7 A. Kumar, S. S. Sun and A. J. Lees, *Coord. Chem. Rev.*, 2008, **252**, 922–939.
8 L. A. Oro, M. A. Ciriano, J. J. Pérez-Torrente and B. E. Villarroya, *Coord. Chem. Rev.*, 1999, **193–195**, 941–975.
9 S. Komeda, M. Lutz, A. L. Spek, M. Chikuma and J. Reedijk, *Inorg. Chem.*, 2000, **39**, 4230–4236.
10 S. Komeda, M. Lutz, A. L. Spek, Y. Yamanaka, T. Sato, M. Chikuma and J. Reedijk, *J. Am. Chem. Soc.*, 2002, **124**, 4738–4746.
11 S. Teletchea, S. Komeda, J. M. Teuben, M. A. Elizondo-Riojas, J. Reedijk and J. Kozelka, *Chem.–Eur. J.*, 2006, **12**, 3741–3753.
12 S. W. Lai, M. C. W. Chan, K. K. Cheung, S. M. Peng and C. M. Che, *Organometallics*, 1999, **18**, 3991–3997.
13 Y. C. Chou, S. F. Huang, R. Koner, G. H. Lee, Y. Wang, S. Mohanta and H. H. Wei, *Inorg. Chem.*, 2004, **43**, 2759–2761.
14 J. M. Casas, J. Forniés, A. Martín and A. J. Rueda, *Organometallics*, 2002, **21**, 4560–4563.
15 J. M. Casas, B. E. Diosdado, J. Forniés, A. Martín, A. J. Rueda and A. G. Orpen, *Inorg. Chem.*, 2008, **47**, 8767–8775.
16 CCDC CSD version 5.30, November 2008 + 3 updates.
17 C. De Haro, G. García, G. Sánchez and G. López, *J. Chem. Res. (S)*, 1986, 119.
18 G. López, J. Ruiz, G. García, C. Vicente, J. M. Martí, J. A. Hermoso, A. Vegas and M. Martínez-Ripoll, *J. Chem. Soc., Dalton Trans.*, 1992, 53–58.
19 D. A. Long and D. Steele, *Spectrochim. Acta*, 1963, **19**, 1955.
20 E. Maslowski, *Vibrational Spectra of Organometallic Compounds*, Wiley, New York, 1977, p. 437.
21 J. Ruiz, N. Cutillas, C. Vicente, M. D. Villa, G. López, J. Lorenzo, F. X. Avilés, V. Moreno and D. Bautista, *Inorg. Chem.*, 2005, **44**, 7365–7376.
22 J. Ruiz, V. Rodríguez, N. Cutillas, G. López and D. Bautista, *Inorg. Chem.*, 2008, **47**, 10025–10036.
23 J. Ruiz, M. D. Villa, N. Cutillas, G. López, D. Bautista, V. Moreno and L. Valencia, *Inorg. Chem.*, 2008, **47**, 4490.
24 G. López, J. Ruiz, C. Vicente, J. M. Martí, G. García, P. A. Chaloner and P. B. Hitchcock, *Organometallics*, 1992, **11**, 4090.
25 $C_{26}H_{12}F_{10}N_4Pd$, FW = 676.80 g mol^{-1}, triclinic, $P\bar{1}$, a = 9.553(1), b = 11.194(1), c = 12.878(1) Å, α = 103.14(1)°, β = 102.51(1)°, γ = 102.98(1)°, V = 1253.7(2) $Å^3$, Z = 2, T = 293 K, needle-shaped crystals, 24 552 measured reflections (R_{int} = 0.0953), 4382 unique, 2749 observed, R_1 = 0.11 ($I > 2\sigma(I)$), wR_2 = 0.35 (all data).
26 G. López, J. Ruiz, G. García, C. Vicente, J. Casabo, E. Molins and C. Miravitlles, *Inorg. Chem.*, 1991, **30**, 2605–2610.
27 M. C. Etter, J. C. MacDonald and J. Bernstein, *Acta Crystallogr., Sect. B: Struct. Sci.*, 1990, **46**, 256–262.
28 M. C. Etter, *Acc. Chem. Res.*, 1990, **23**, 120–126.
29 M. C. Etter, *J. Phys. Chem.*, 1991, **95**, 4601–4610.
30 C. Janiak, *J. Chem. Soc., Dalton Trans.*, 2000, 3885–3896.
31 G. Althoff, J. Ruiz, V. Rodríguez, G. López, J. Pérez and C. Janiak, *CrystEngComm*, 2006, **8**, 662–665.
32 V. R. Vangala, A. Nangia and V. M. Lynch, *Chem. Commun.*, 2002, 1304–1305.

33 F. Babudri, G. M. Farinola, F. Naso and R. Ragni, *Chem. Commun.*, 2007, 1003–1022.
34 K. Kasai and M. Fujita, *Chem.–Eur. J.*, 2007, **13**, 3089–3105.
35 J. Ruiz, M. D. Villa, V. Rodríguez, N. Cutillas, C. Vicente, G. López and D. Bautista, *Inorg. Chem.*, 2007, **46**, 5448–5449.
36 M. Nishio, *CrystEngComm*, 2004, **6**, 130–158.
37 J. Ruiz, J. Lorenzo, C. Vicente, G. López, J. M. López-De-Luzuriaga, M. Monge, F. X. Avilés, D. Bautista, V. Moreno and A. Laguna, *Inorg. Chem.*, 2008, **47**, 6990–7001.
38 J. Ruiz, M. T. Martínez, F. Florenciano, V. Rodríguez, G. López, J. Pérez, P. A. Chaloner and P. B. Hitchcock, *Inorg. Chem.*, 2003, **42**, 3650–3661.
39 J. Ruiz, M. T. Martínez, F. Florenciano, V. Rodríguez, G. López, J. Pérez, P. A. Chaloner and P. B. Hitchcock, *Dalton Trans.*, 2004, 929–932.
40 R. G. Parr and W. Yang, *Density Functional Theory of Atoms and Molecules*, Oxford University Press, Oxford, 1989.
41 (*a*) P. K. Chattaraj, H. Lee and R. G. Parr, *J. Am. Chem. Soc.*, 1991, **113**, 1855–1856; (*b*) A. Cedillo, P. K. Chattaraj and R. G. Parr, *Int. J. Quantum Chem.*, 2000, **77**, 403–407.
42 R. G. Pearson, *J. Am. Chem. Soc.*, 1963, **85**, 3533–3539.
43 See for instance: A. Ponti and G. Molteni, *Chem.–Eur. J.*, 2006, **12**, 1156–1161; and references cited therein.
44 R. G. Parr and W. Yang, *J. Am. Chem. Soc.*, 1984, **106**, 4049–4050.
45 (*a*) S. Damoun, G. Van de Woude, F. Méndez and P. Geerlings, *J. Phys. Chem. A*, 1997, **101**, 886–893; (*b*) A. Ponti, *J. Phys. Chem. A*, 2000, **104**, 8843–8846.
46 A. Espinosa, A. Frontera, R. García, M. A. Soler and A. Tárraga, *Arkivoc*, 2005, **(ix)**, 415–437.
47 R. G. Parr, L. V. Szentpaly and S. Liu, *J. Am. Chem. Soc.*, 1999, **121**, 1922–1924.
48 F. De Proft, W. Langenaeker and P. Geerlings, *J. Phys. Chem.*, 1993, **97**, 1826–1831; F. De Proft, S. Amira, K. Choho and P. Geerlings, *J. Phys. Chem.*, 1994, **98**, 5227–5233; S. Kishnamurty and S. Pal, *J. Phys. Chem. A*, 2000, **104**, 7639–7645.
49 R. Parthasarathi, J. Padmanabhan, M. Elango, V. Subramanian and P. K. Chattaraj, *Chem. Phys. Lett.*, 2004, **394**, 225–230.
50 The species **7** has been obtained by constrained optimization keeping all donor atoms co-planar with the Pt centre and orthogonal angles between the central C_6F_5 ligand and the peripheral ones.
51 The above parameters are directly related with kinetic aspects as they concern the very first stage of the interaction between (pairs of) reactive sites in both reactants. Consequently they reflect how much the system is destabilized at the beginning of the interaction and therefore give an insight about the energy content of the transition state (TS).
52 R. F. W. Bader, *Atoms in Molecules: A Quantum Theory*, Oxford University Press, Oxford, 1990.
53 J. M. Casas, J. Forniés, A. Martín, V. M. Orera, A. G. Orpen, A. J. Rueda, B. E. Diosdado and A. G. Orpen, *Inorg. Chem.*, 1995, **34**, 6514–6519.
54 The antibonding nature of the HOMO has been corroborated by *in silico* one-electron oxidation of this compound that yields the radical-cation derivative $\mathbf{6}^+$ featuring a shorter Pt–Pt contact ($d_{Pt\cdots Pt} = 2.845$ Å) with remarkable bonding character (WBI 0.185; $\rho(\mathbf{r}_c) = 0.0437$ e/a_o^3).
55 M. D. Meijer, A. W. Kleij, B. S. Williams, D. Ellis, M. Lutz, A. L. Spek, G. P. M. van Klink and G. van Koten, *Organometallics*, 2002, **21**, 264–271.
56 J. Ruiz, V. Rodríguez, N. Cutillas, A. Hoffmann, A.-C. Chamayou, K. Kazmierczak and C. Janiak, *CrystEngComm*, 2008, **10**, 1928–1938.
57 H. Hosseini Monfared, J. Sanchiz, Z. Kalantari and C. Janiak, *Inorg. Chim. Acta*, 2009, **362**, 3791–3795.
58 A.-C. Chamayou, C. Biswas, A. Ghosh and C. Janiak, *Acta Crystallogr., Sect. C: Cryst. Struct. Commun.*, 2009, **65**, m311.
59 J. P. Macquet and J. L. Butour, *Biochimie*, 1978, **60**, 901–914.
60 V. Brabec, V. Kleinwächter, J. Butour and M. P. Johnson, *Biophys. Chem.*, 1990, **35**, 129–141.
61 G. Cervantes, M. J. Prieto and V. Moreno, *Met.-Based Drugs*, 1997, **4**, 9.
62 G. Cervantes, S. Marchal, M. J. Prieto, J. M. Pérez, V. M. González, C. Alonso and V. Moreno, *J. Inorg. Biochem.*, 1999, **77**, 197–203.
63 J. Ruiz, C. Vicente, C. de Haro and D. Bautista, *Dalton Trans.*, 2009, 5071–5073.
64 H. M. Ushay, T. D. Tullius and S. J. Lippard, *Biochemistry*, 1981, **20**, 3744–3748.
65 S. Y. Loh, P. Mistry, L. R. Kelland, G. Abel and K. R. Harrap, *Br. J. Cancer*, 1992, **66**, 1109–1115.
66 P. M. Goddard, R. M. Orr, M. R. Valenti, C. F. Barnard, B. A. Murrer, L. R. Kelland and K. R. Harrap, *Anticancer Res.*, 1996, **16**, 33–38.
67 B. C. Behrens, T. C. Hamilton, H. Masuda, K. R. Grotzinger, J. Whang-Peng, K. G. Louie, T. Knutsen, W. M. McKoy, R. C. Young and R. F. Ozols, *Cancer Res.*, 1987, **47**, 414–418.
68 L. R. Kelland, C. F. J. Barnard, K. J. Mellish, M. Jones, P. M. Goddard, M. Valenti, A. Bryant, B. A. Murrer and K. R. Harrap, *Cancer Res.*, 1994, **54**, 5618–5622.
69 G. M. Sheldrick, *SHELXS-97, SHELXL-97, Programs for Crystal Structure Analysis*, University of Göttingen, Germany, 1997.
70 H. D. Flack, *Acta Crystallogr., Sect. A: Found. Crystallogr.*, 1983, **39**, 876–881.
71 K. Brandenburg, *Diamond (Version 3.1f), Crystal and Molecular Structure Visualization, Crystal Impact*, K. Brandenburg and H. Putz Gbr, Bonn (Germany) 2007, http://www.crystalimpact.com/diamond.
72 A. L. Spek, *J. Appl. Crystallogr.*, 2003, **36**, 7; *PLATON—A Multipurpose Crystallographic Tool*, Utrecht University, Utrecht, The Netherlands, A. L. Spek, (2008); *Windows implementation*, L. J. Farrugia, University of Glasgow, Scotland, Version 40608 (2008).
73 X.-J. Yang, F. Drepper, B. Wu, W.-H. Sun, W. Haehnel and C. Janiak, *Dalton Trans.*, 2005, 256–267; and supplementary material therein.
74 L. J. Bartolottiand and K. Fluchick, in *Reviews in Computational Chemistry*, ed. K. B. Lipkowitz and B. D. Boyd, VCH, New York, 1996, vol. 7, pp. 187–216.
75 P. R. Rablen, J. W. Lockman and W. L. Jorgensen, *J. Phys. Chem. A*, 1998, **102**, 3782–3797.
76 M. J. Frisch, G. W. Trucks, H. B. Schlegel, G. E. Scuseria, M. A. Robb, J. R. Cheeseman, J. A. Montgomery, Jr., T. Vreven, K. N. Kudin, J. C. Burant, J. M. Millam, S. S. Iyengar, J. Tomasi, V. Barone, B. Mennucci, M. Cossi, G. Scalmani, N. Rega, G. A. Petersson, H. Nakatsuji, M. Hada, M. Ehara, K. Toyota, R. Fukuda, J. Hasegawa, M. Ishida, T. Nakajima, Y. Honda, O. Kitao, H. Nakai, M. Klene, X. Li, J. E. Knox, H. P. Hratchian, J. B. Cross, V. Bakken, C. Adamo, J. Jaramillo, R. Gomperts, R. E. Stratmann, O. Yazyev, A. J. Austin, R. Cammi, C. Pomelli, J. Ochterski, P. Y. Ayala, K. Morokuma, G. A. Voth, P. Salvador, J. J. Dannenberg, V. G. Zakrzewski, S. Dapprich, A. D. Daniels, M. C. Strain, O. Farkas, D. K. Malick, A. D. Rabuck, K. Raghavachari, J. B. Foresman, J. V. Ortiz, Q. Cui, A. G. Baboul, S. Clifford, J. Cioslowski, B. B. Stefanov, G. Liu, A. Liashenko, P. Piskorz, I. Komaromi, R. L. Martin, D. J. Fox, T. Keith, M. A. Al-Laham, C. Y. Peng, A. Nanayakkara, M. Challacombe, P. M. W. Gill, B. G. Johnson, W. Chen, M. W. Wong, C. Gonzalez and J. A. Pople, *GAUSSIAN 03 (Revision B.03)*, Gaussian, Inc., Wallingford, CT, 2004.
77 (*a*) Y. Zhao and D. G. Truhlar, *J. Phys. Chem. A*, 2004, **108**, 6908–6918; (*b*) Y. Zhao and D. G. Truhlar, *J. Phys. Chem. A*, 2005, **109**, 5656–5667.
78 For instance, see: J. Muñiz, L. E. Sansores, A. Martínez and R. Salcedo, *THEOCHEM*, 2007, **820**, 141–147.
79 K. Wiberg, *Tetrahedron*, 1968, **24**, 1083–1096.
80 (*a*) AIM2000 v. 2.0, designed by F. W. Biegler-König and J. Schönbohm, 2002. Home page http://www.aim2000.de/F. Biegler-König, J. Schönbohm and D. J. Bayles, *J. Comput. Chem.*, 2001, **22**, 545–559; (*b*) F. Biegler-König and J. Schönbohm, *J. Comput. Chem.*, 2002, **23**, 1489–1494.